

Solution- and Solid-state Stereochemistry of (–)- α -Lobeline Hydrochloride and Hydrobromide, a Respiratory-stimulant Drug

Robert Glaser,^{a,*} Paul Hug,^b Marc Drouin and André Michel^c

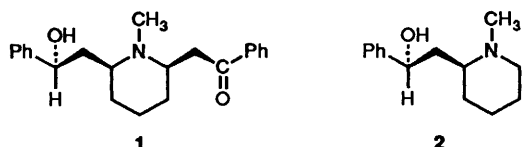
^a Department of Chemistry, Ben-Gurion University of the Negev, Beer-Sheva 84105, Israel

^b Ciba-Geigy AG, CH-4002 Basel, Switzerland

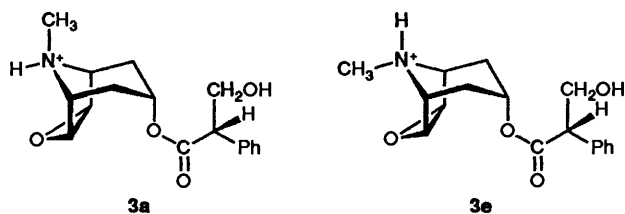
^c Département de Chimie, Université de Sherbrooke, Sherbrooke, Québec, Canada J1K 2R1

The solid-state structure of (–)- α -lobeline hydrobromide has been determined by single crystal X-ray diffraction analysis. (–)- α -Lobeline hydrobromide gives crystals belonging to the orthorhombic $P2_12_1$ space group, and at 298 K: $a = 6.0100(3)$, $b = 11.7177(4)$, $c = 28.977(2)$ Å, $V = 2040.7(2)$, $Z = 4$, $R(F) = 0.030$, and $R_w(F) = 0.022$. The (2*R*,6*S*,*C*₈*S*)-absolute configuration was determined from the effects of anomalous dispersion of the bromine atom. The *N*-methyl group exists in an axial configuration similar to that previously described for the hydrochloride salt. However, in the hydrobromide salt the β -hydroxyphenethyl residue exhibits a different conformation from that noted for the hydrochloride salt. ¹H and ¹³C NMR spectroscopy for the hydrochloride salt dissolved in CD₂Cl₂ shows axial- and equatorial-*N*-methyl solution-state diastereoisomers in the ratio *ca.* 5:1, respectively. The major contributors to the time-averaged structures of the salt in D₂O and the free base in CDCl₃ also show axial *N*-methyl orientations. Conformational differences for the acetophenonyl and β -hydroxyphenethyl moieties were found in the two *N*-methyl epimers, as well as in the time-averaged salt (D₂O) and free base (CDCl₃) structures. The putative bioactive conformation of the nicotine agonist was found to have a different acetophenonyl arm conformation than that found in both crystals.

The nicotine agonist (2*R*,6*S*,*C*₈*S*)-(–)- α -lobeline {(–)-2-[6-(β -hydroxyphenethyl)-1-methyl-2-piperidyl]acetophenone, **1**} is a natural product isolated from *Lobelia inflata* L, and *Lobeliaceae* (Indian tobacco).¹ It is structurally related to the sedum alkaloid (2*S*,*C*₈*S*)-(–)-sedamine [(–)-2- β -hydroxyphenethyl-1-methylpiperidine, **2**].² The hydrochloride salt of the lobelia alkaloid is utilized therapeutically as a respiratory-stimulant.¹



Recently, the X-ray crystallographic structure determination of (–)- α -lobeline hydrochloride monohydrate (1·HCl·H₂O) was reported by Barlow and Johnson.³ In the solid-state, 1·HCl·H₂O exhibits an axially-oriented *N*-methyl group.³ An axial *N*-methyl is also found in crystalline (*Nr*,*C*₈-*S*)-(–)-scopolamine hydrobromide (anhydrous⁴ and hemihydrate⁵ forms), **3a**.



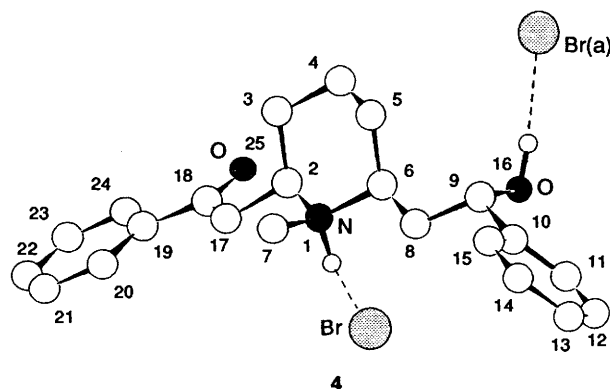
¹H NMR spectra of appropriately *N*-substituted azacyclic salts (e.g. tropane alkaloid salts like scopolamine HBr), show equatorial (**3e**) and axial (**3a**) *N*-methyl diastereoisomers at the slow exchange limit (SEL) for prototropic shift/nitrogen inversion in CD₂Cl₂ or in acidic aqueous solution.⁷ For some alkaloid salts (e.g. atropine sulfate)^{6,7} the relatively large

dispersion of ¹³C chemical shifts enables recording of ¹³C NMR SEL spectra even in neutral D₂O. Using ¹³C NMR spectroscopy, the ratio of axial:equatorial *N*-methyl scopolamine HBr diastereoisomers was found to be strongly solvent dependent (*ca.* 19:1 **3a**:**3e** in D₂O and *ca.* 1:19 **3a**:**3e** in CD₂Cl₂).⁶

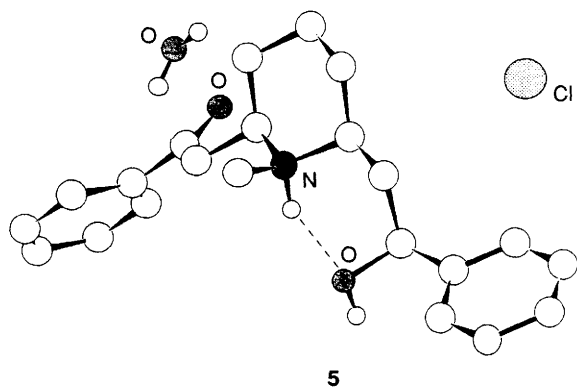
This paper reports the solution-state stereochemistry of (–)- α -lobeline hydrochloride salt (1·HCl·H₂O) and free base, their solution- and solid-state ¹H and ¹³C NMR spectral parameters, plus the X-ray crystallographically-determined solid-state stereochemistry and absolute configuration of the corresponding hydrobromide salt (1·HBr).

Results and Discussion

X-Ray Diffraction Studies.—(–)- α -Lobeline hydrobromide (1·HBr) gave crystalline prisms belonging to the orthorhombic



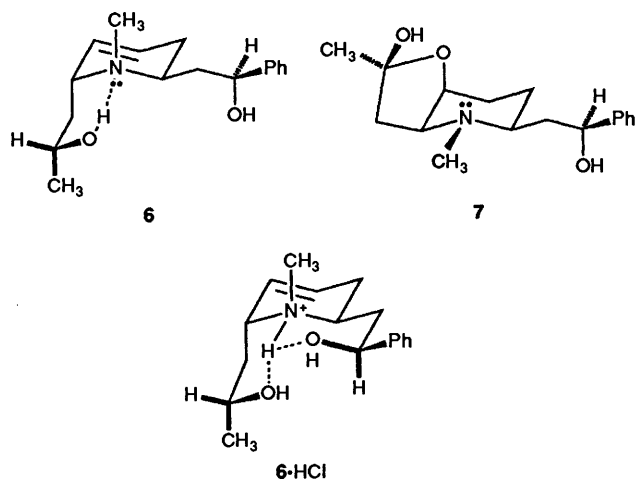
$P2_12_1$ space group. The numbering scheme for the skeleton is depicted in structure 4. The atomic parameters x , y and z are listed in Table 4, while bond distances and angles are given in Table 5, and torsion angles are reported in Table 6. Tables of thermal parameters and hydrogen atom coordinates have been



deposited at the Cambridge Crystallographic Data Centre (CCDC).*

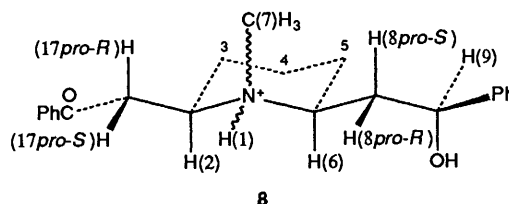
Determination of (1*R*,2*R*,6*S*,*C_β**S*)-absolute configuration was based on the effects of anomalous dispersion from the bromine atom.⁸ The (2*R*,6*S*,*C_β**S*)-absolute configuration of **1** had previously been chemically correlated with (2*S*,*C_β**S*)-(-)-sedamine⁹ (**2**) by Schoepf and Mueller.² Crystalline **1**·HBr was found to also exhibit an axial *N*-methyl group similar to **1**·HCl·H₂O. The solid-state molecular geometry of **1**·HBr showed some conformational differences compared to that of **1**·HCl·H₂O (see structures **4** and **5**). Primary differences involved the conformation about the C(6)–C(8) bond in the β-hydroxyphenethyl arm, *i.e.* torsion angles N(1)–C(6)–C(8)–C(9) [177.5° (**1**·HBr) and 60.1° (**1**·HCl·H₂O)] and C(5)–C(6)–C(8)–C(9) [55.8° (**1**·HBr) and –173.4° (**1**·HCl·H₂O)]. Minor differences were noted involving carbonyl moiety coplanarity with the benzoyl phenyl ring [*e.g.* torsion angle C(17)–C(18)–C(19)–C(20) –1.1° (**1**·HBr) and 41.4° (**1**·HCl·H₂O)]. Perusal of Table 6 shows all other corresponding torsion angles to have very similar values in both molecules. Therefore, the **1**·HBr and **1**·HCl·H₂O molecular geometries represent two of the three staggered rotamers about the C(6)–C(8) bond, and they may be respectively assigned antiperiplanar and (+)-synclinal conformational descriptors based on torsion angle N(1)–C(6)–C(8)–C(9). An intramolecular hydrogen bond is noted in the **1**·HCl·H₂O rotamer [N⁺–H...O(H)], while the bromide anion in the **1**·HBr unit cell (see structure **4**) provides an intermolecular hydrogen-bonding bridge [*i.e.* N⁺–H...Br[–]...H–O] between the N⁺–H(1) proton in one molecule and the O–H(16) proton in a second molecule. The same antiperiplanar and (+)-synclinal β-hydroxyphenethyl moiety conformational archetypes have also been found in the X-ray crystallographically determined structures of related sedum alkaloids (–)-sedinine¹⁰ (**6**), (–)-sedacryptine¹¹ (**7**), and (–)-sedinine hydrochloride^{10,†} (**6**·HCl).

Regular intramolecular hydrogen-bonds were located in solid state free bases **6** and **7**, while a bifurcated hydrogen-bonding arrangement is apparent in crystalline **6**·HCl. Axial *N*-methyl groups were observed in both solid-state (–)-sedinine free base and hydrochloride salt; and an equatorially oriented *N*-methyl group was seen in crystalline (–)-sedacryptine free base.^{10,11} Conformations about the C(8)–C(9) and C(9)–C(10) bonds in the β-hydroxyphenethyl arm are very similar in X-ray structures **1**·HBr, **1**·HCl·H₂O, **6** and **7**, *e.g.* C(6) is (–)-synclinally orientated to O(16) [angle C(6)–C(8)–C(9)–O(16):



–54.2°, –74.3°, –57.1° and –54.0°, respectively (this is also apparent pictorially for **6**·HCl)], and the phenyl ring approximately eclipses O(16) [angle C(11)–C(10)–C(9)–O(16): –14.0°, –8.8°, –31.8° and –21.1°, respectively]. Finally, two acetophenonyl-arm conformational features deserve comment: C(2) eclipses O(25), and N(1) is approximately antiperiplanar to C(18) in both X-ray structures **4** and **5** [angle C(6)–C(7)–C(8)–O(25): 8.6° and –5.8°, respectively; angle C(6)–C(7)–C(8)–O(25): –159.5° and –152.0°, respectively].

¹H and ¹³C NMR SEL Studies on the Salt.—¹H and ¹³C NMR SEL spectral parameters for a mixture of α-lobeline hydrochloride *N*-methyl diastereoisomers **1a,e**·HCl [and fast exchange limit (FEL) parameters for both salt **1**·HCl and free base **1**] are listed in Tables 1 and 2. The proton numbering diagram is given in structure **8**.



Two species in the ratio of *ca.* 5:1 were clearly seen in both ¹H and ¹³C NMR spectra of α-lobeline hydrochloride dissolved in CD₂Cl₂. Axial and equatorial descriptors were assigned to the *N*-methyl group orientation in the respective major and minor solution-state species, based on magnitudes of coupling constants involving the N–H proton and its vicinal neighbours on the piperidine ring. Resonances from methine and methylene protons in the phenethyl moiety were readily identified as the A-part of an apparent AMX 3-spin system, and the MR-part of an apparent AMRX 4-spin system giving four and eight transition multiplets, respectively. Similarly, methylene protons in the acetophenonyl moiety were easily ascertained as the AM-part of an apparent AMX 3-spin system.

Each piperidinyl ring methine proton appeared as the A-part of an apparent AFIMRX 6-spin system. The major species H(2) resonance appeared as a 32-transition multiplet of 13 lines in the ratio of 1:3:3:1:1:4:6:4:1:1:3:3:1. The order of the transitions is 1,[2,3,5],[4,6,7],8,9,[10,11,13,17],[12,14,15,18,19,21],[16,20,22,23],24,25,[26,27,29],[28,30,31],32 due to 16 overlaps since $J(\text{H2-H17pro-S}) \approx J(\text{H2-H3eq}) \approx J(\text{H1-H2})$ and three overlaps since $J(\text{H2-H3ax}) \approx [(J\text{H2-H17pro-S}) + J(\text{H2-H17pro-R})]$. The major species H(6) resonance was seen as a 32-transition multiplet of 11-lines in the ratio of 1:2:3:4:4:4:

* For details of the CCDC deposition scheme, see 'Instructions for Authors (1992)' in the January issue of *J. Chem. Soc., Perkin Trans. 2*, 1992.

† Coordinates for **6**·HCl are not resident in the Cambridge Crystallographic Data Base; however, the β-hydroxyphenethyl moiety conformation is clearly depicted and discussed in ref. 10.

Table 1 ^1H NMR SEL spectral parameters for the mixture of (1*S*,2*R*,6*S*,*C}_\beta\text{S})-equatorial- and (1*R*,2*R*,6*S*,*C}_\beta\text{S})-axial-*N*-methyl (–)- α -lobeline hydrochloride diastereoisomers (1*a*·HCl); and *N*-methyl isomer FEL interconversion parameters for the salt (1·HCl) and the corresponding free base (1)**

| | 1 <i>a</i> ·HCl ^b (major species) | 1 <i>e</i> ·HCl ^b (minor species) | 1·HCl ^c | 1 ^d |
|----------------------------------|---|---|--------------------|---------------------|
| δ_{H} ^a | | | | |
| H(1) | 11.19 | 11.57 | — | — |
| H(2) | 4.13 | 3.79 | 3.96 | 3.58 |
| H(3ax) | 1.56 | — | — | — |
| H(3eq) | 1.99 | — | — | — |
| H(4ax) | ~1.91 | — | — | — |
| H(4eq) | ~1.91 | — | — | — |
| H(5ax) | 1.63 | — | — | — |
| H(5eq) | 1.87 | — | — | — |
| H(6) | 3.89 | 3.29 | 3.79 | 3.24 |
| H(7) | 2.77 | 2.69 | 2.64 | 2.36 |
| H(8 <i>pro-R</i>) | 2.32 ₁ | 2.32 ₇ | — | 1.94 |
| H(8 <i>pro-S</i>) | 1.74 | 2.13 | — | — |
| H(9) | 4.95 | 4.88 | 4.90 | 4.95 |
| H(17 <i>pro-R</i>) | 3.10 | 3.42 ^e | 3.43 | 3.03 ^e |
| H(17 <i>pro-S</i>) | 4.06 | 4.03 ^e | 3.50 | 3.23 ^e |
| $J(\text{H-H})$ ^f | | | | |
| 1–2 | 2.5(1) | 8.6(3) | — | — |
| 1–6 | 3.0(3) | 8.9(1) | — | — |
| 1–7 | 5.3(1) | 4.9(1) | — | — |
| 2–3ax | 12.9(1) | 11.5(8) | — | 11.1(2) |
| 2–3eq | 2.5(1) | 2.9(5) | — | 2.9(5) |
| 2–17 <i>pro-R</i> | 10.5(2) | 5.1(1) | 9.2(1) | 5.0(5) ^e |
| 2–17 <i>pro-S</i> | 2.4(1) | 5.1(1) | 5.0(1) | 8.2(4) ^e |
| 5ax–6 | 12.3(2) | 11.9(1) | — | — |
| 5eq–6 | 3.0(3) | 3.2(1) | — | 2.6(2) |
| 6–8 <i>pro-R</i> | 6.8(1) | 3.0(1) | — | 11.0(1) |
| 6–8 <i>pro-S</i> | 6.0(2) | 9.2(1) | — | 2.6(2) |
| 8 <i>pro-R</i> –8 <i>pro-S</i> | –14.8(1) | –14.2(1) | — | –14.7(1) |
| 8 <i>pro-R</i> –9 | 10.9(1) | 10.7(1) | 9.9(1) | 10.7(1) |
| 8 <i>pro-S</i> –9 | 2.1(1) | 2.9(1) | 2.4(1) | 2.7(1) |
| 17 <i>pro-R</i> –17 <i>pro-S</i> | –16.5(1) | –19.0(1) | –18.6(4) | –15.9(2) |

^a 400 MHz, 298 K. ^b ppm downfield from tetramethylsilane, CD₂Cl₂, 5:1 ratio of 1*a*·HCl:1*e*·HCl. ^c ppm downfield from 3-(methylsilyl)-1-propanesulfonic acid, sodium salt, D₂O. ^d ppm downfield from tetramethylsilane, CDCl₃. ^e Assignments may be reversed. ^f Hz, esds in parentheses refer to last digit printed.

4:4:3:2:1. The order of the transitions is 1,[2,3],[4,5,9],[6,7,10,11],[8,12,13,17],[14,15,18,19],[16,20,21,25],[22,23,26,27],[24,28,29],[30,31],32 due to 8 overlaps since $J(\text{H1-H6}) \approx J(\text{H5eq-H6})$, 4 overlaps since $J(\text{H6-H8pro-S}) \approx [J(\text{H1-H6}) + J(\text{H5eq-H6})]$, 4 overlaps since $J(\text{H6-H8pro-R}) \approx [J(\text{H1-H6}) + J(\text{H5eq-H6})]$, and 5 overlaps since $J(\text{H5ax-H6}) \approx [J(\text{H1-H6}) + J(\text{H5eq-H6}) + J(\text{H6-H8pro-S})]$. The minor species H(2) resonance was found as a 32-transition multiplet of 13 lines in the ratio of 1:1:2:3:3:4:4:4:3:3:2:1:1. The order of the transitions is 1,2,[3,5],[4,6,9],[7,10,17],[8,11,13,18],[12,14,19,21],[15,20,22,25],[16,23,26],[24,27,29],[28,30],31,32 due to 8 overlaps since $J(\text{H2-H17pro-R}) \approx J(\text{H2-H17pro-S})$, 6 overlaps since $J(\text{H1-H2}) \approx [J(\text{H2-H3eq}) + J(\text{H2-H17pro-R})]$, and 5 overlaps since $J(\text{H2-H3ax}) \approx [J(\text{H2-H17pro-R}) + J(\text{H2-H17pro-S})]$. Finally, the minor species H(6) resonance was observed as a 32-transition multiplet of 13 lines in the ratio of 1:2:1:2:5:4:2:4:5:2:1:2:1. The order of the transitions is 1,[2,3],4,[5,9],[6,7,10,11,17],[8,12,18,19],[13,20],[14,15,21,25],[16,22,23,26,27],[24,28],29,[30,31],32 due to 8 overlaps since $J(\text{H6-H8pro-R}) \approx J(\text{H5eq-H6})$, 6 overlaps since $J(\text{H1-H6}) \approx J(\text{H6-H8pro-S})$, and 5 overlaps since $J(\text{H5ax-H6}) \approx [J(\text{H6-H8pro-R}) + J(\text{H1-H6})]$. Analyses of transitional order in these multiplets is a non-trivial and crucial process in determining relevant coupling constants. Decoupling of the NH proton in each species simplified each H(2,6) resonance to the corresponding 16-transition multiplet of an apparent 5-spin system, and subsequent analysis confirmed the numerical values of the relevant vicinal coupling constants. Multiple measurements were made of coupling constants in each multiplet, values

were averaged, and estimated standard deviations were determined. While the dispersion of resonances from ^1H nuclei ligated to C(3–5) was insufficient for assignment or analysis in spectra measured in 9.4 and 11.7 T fields, vicinal coupling constants involving H(3ax, eq; 5ax, eq)-nuclei were readily obtained from the H(2,6) multiplets.

COSY-90 2D NMR correlation spectroscopy showed the homonuclear coupling networks [with the exception of H(4ax,4eq) nuclei in the major species, and H(3ax,3eq,4ax,4eq,5ax,5eq) nuclei in the minor species]. COSY-90 cross-peaks involving H(2) and H(3ax,eq) [or H(6) and H(5ax,eq)] were markedly different in terms of width. Since vicinal coupling constant magnitudes involving these nuclei were *ca.* 12–13 Hz and *ca.* 2–3 Hz (characteristic of antiperiplanar and synclinal arrangements, respectively), the H(3) [or H(5)] nucleus affording the wider cross-peak was assigned an axial descriptor while that giving the narrower cross-peak was assigned an equatorial orientation. ^{13}C NMR resonance multiplicity was ascertained by the DEPT pulse sequence [90° and 135° pulse angles]. XHCORR 2D NMR heteronuclear correlation spectroscopy enabled assignment of all major species ^{13}C NMR resonances. Since all major species of aliphatic ^{13}C nuclei [with the exception of C(4)] were readily correlated with previously assigned ^1H nuclei, the one remaining CH₂ cross-peak [δ_{C} 22.65 \longleftrightarrow δ_{H} 1.91] was assigned to C(4)/H(4ax,eq). Minor species C(2,6,7,9) assignments were also forthcoming from this spectrum. Aromatic ^{13}C nuclei were assigned by analogy to corresponding peaks in acetophenone and α -methylbenzyl alcohol.¹² *pro-R/pro-S* descriptors were assigned by the

Table 2 ^{13}C NMR SEL spectral parameters for the mixture of (1*S*,2*R*,6*S*, C_{β} *S*)-equatorial- and (1*R*,2*R*,6*S*, C_{β} *S*)-axial-*N*-methyl (–)- α -lobeline hydrochloride diastereoisomers (**1e**·HCl) (CP-MAS recorded values for crystalline **1a**·HCl in square brackets); and FEL spectral parameters for the salt (**1**·HCl) and the corresponding free base (**1**)

| | 1a ·HCl ^b [solid-state] (major solution-species) | 1e ·HCl ^b (minor solution-species) | 1 ·HCl ^c | 1 ^d (free base) |
|--------------|---|---|----------------------------|--------------------------------------|
| δ_c^a | | | | |
| C(2) | 60.81 [61.38] | 62.40 | 60.27 | 59.06 |
| C(3) | 23.71 [23.80] | 29.33 | 22.41 | 23.46 |
| C(4) | 22.65 [21.92] | 22.76 | 21.45 | 23.30 |
| C(5) | 24.45 [25.68] | 31.14 | 22.49 | 24.76 |
| C(6) | 63.87 [66.39 ^e] | 65.21 | 64.35 | 64.56 |
| C(7) | 27.30 [30.90] | 38.03 | 25.52 | 27.33 |
| C(8) | 42.00 [41.73 ^f] | 41.85 | 38.24 | 43.81 |
| C(9) | 70.91 [66.39 ^e] | 70.12 | 72.14 | 75.76 |
| C(10) | 144.78 [145.98 ^g] | 144.29 | 142.66 | 145.09 |
| C(11,15) | 125.64 [— ^h] | 125.79 | 125.17 | 125.53 |
| C(12,14) | 128.52 ^e [— ^h] | 128.65 ^g | 127.72 ^g | 128.12 ^g |
| C(13) | 127.45 [— ^h] | 127.82 | 127.62 | 126.99 |
| C(17) | 40.58 [41.73 ^f] | 40.90 | 37.53 | 40.48 |
| C(18) | 195.42 [195.37] | 196.51 | 200.56 | 198.20 |
| C(19) | 136.26 [144.94 ^g] | 135.94 | 134.74 | 137.02 |
| C(20,24) | 128.42 ^e [— ^h] | 128.48 ^g | 128.31 ^g | 128.23 ^g |
| C(21,23) | 128.92 ^e [— ^h] | 128.99 ^g | 128.42 ^g | 128.71 ^g |
| C(22) | 133.93 [— ^h] | 134.10 | 134.19 | 133.17 |

^a 100 MHz (75.3 MHz for CP-MAS), 298 K. ^b ppm downfield from tetramethylsilane, CD_2Cl_2 , 5:1 ratio of **1a**·HCl:**1e**·HCl. ^c ppm downfield from 3-(methylsilyl)-1-propanesulfonic acid, sodium salt, D_2O . ^d ppm downfield from tetramethylsilane, CDCl_3 , one primary species observed in 100 MHz spectrum with traces of a second [e.g. CH_3 resonances: δ 27.33 and 35.69 (trace) at 298 K], three solution-state species for **1** observed at 50.3 MHz [e.g. CH_3 resonances: δ 27.18, 35.66, and 40.88 in the ratio of ca. 17:5:4 at 298 K], major species 100 MHz data presented in above table, other unassigned minor species resonances: CH_2 δ 44.34, 43.24, 38.79, 33.54, 32.94, 23.85, 22.86, 20.50; CH δ 68.36, 61.00, 59.88, 51.50. ^e C(6,9) not resolved, single broadened resonance. ^f C(8,17) resonances not resolved. ^g Assignments may be interchanged. ^h Unassigned aromatic CH resonances: 135.91, 132.90 [low intensity], 128.06 [double intensity], 126.22.

Table 3 Crystallographic details for (1*R*,2*R*,6*S*, C_{β} *S*)-(–)- α -lobeline hydrobromide (**1**·HBr)

| | |
|--|---|
| Formula | $\text{C}_{22}\text{H}_{25}\text{NO}_2\text{Br}$ |
| <i>M</i> | 415.35 |
| Space group | $P2_12_12_1$ |
| <i>a</i> /Å | 6.0100(3) |
| <i>b</i> /Å | 11.7177(4) |
| <i>c</i> /Å | 28.977(2) |
| <i>V</i> /Å ³ | 2040.7(2) |
| <i>Z</i> | 4 |
| $\rho_{\text{calc}}/\text{g cm}^{-3}$ | 1.352 |
| Linear absorption coefficient/cm ⁻¹ | 28.6 |
| Temperature/K | 293 |
| Crystal size/mm | 0.22 × 0.22 × 0.35 |
| Radiation | Graphite-monochromated Cu $K_{\alpha\text{AV}}$ ($\lambda = 1.5418 \text{ \AA}$) |
| Collection range | + <i>h</i> , + <i>k</i> , + <i>l</i> $0 \leq h \leq 6, 0 \leq k \leq 13, 0 \leq l \leq 35$ |
| 2 θ limits | $3^\circ \leq 2\theta \leq 143.29^\circ$ |
| Scan type | $\theta/2\theta$ |
| Scan width/deg | $1.0 + 0.25 \tan\theta$ |
| Scan speed/deg min ⁻¹ | 2.7 |
| Scan speed for Friedel pair collection/deg min ⁻¹ | 1.33 |
| Background time/scan time | 0.33 |
| Unique data | 2271 |
| Unique data with $I_{\text{net}} \geq 2.0\sigma(I_{\text{net}})$ | 2130 |
| No. of variables | 236 |
| <i>R</i> (<i>F</i>) | 0.030 |
| <i>R</i> _w (<i>F</i>) | 0.022 |
| Weighting factor, <i>w</i> | $(\sigma F_{\text{obs}})^{-2}$ |
| Goodness of fit | 2.43 |

^a Goodness of fit = $[\sum_i \{w_i(|F_{\text{obs}i}| - |F_{\text{calc}i}|)^2\} / (\text{no. of reflections} - \text{no. of parameters})]^{1/2}$.

homonuclear difference–nuclear Overhauser effect (NOED-IFF), *vide infra*.

Only three of the minor-species H(8*pro-R*) resonance eight lines were observed due to overlapping of the major-species H(8*pro-R*) resonance. A homonuclear decoupling difference experiment { δ 3.29, minor species H(6)} afforded all eight

lines. Assignments of ^1H and ^{13}C nuclei in the FEL spectra of the salt and free base were made in an analogous manner. In general, the dispersion of chemical shifts in these spectra were less amenable to complete spectral assignment.

Nuclei C(2,3,17) in the acetophenonyl half of the molecule were shifted upfield by an average of 2(1) ppm in the major

Table 4 Non-hydrogen atomic parameters for (1*R*,2*R*,6*S*,*C*₈*S*)-(-)- α -lobeline hydrobromide (1·HBr); esds in parentheses refer to last digit printed^a

| Atom | x | y | z |
|-----------------|-------------|-------------|-------------|
| Br ^b | 0.313 87(8) | 0.214 00(3) | 0.679 31(1) |
| N(1) | 0.055 0(4) | 0.444 9(2) | 0.704 33(8) |
| C(2) | 0.124 5(5) | 0.500 2(3) | 0.658 78(9) |
| C(3) | 0.114 9(6) | 0.629 2(3) | 0.662 3(1) |
| C(4) | 0.256 0(6) | 0.672 2(2) | 0.701 7(1) |
| C(5) | 0.188 8(6) | 0.617 3(3) | 0.746 9(1) |
| C(6) | 0.198 8(6) | 0.488 2(2) | 0.743 89(9) |
| C(7) | -0.191 3(6) | 0.450 7(3) | 0.713 2(1) |
| C(8) | 0.143 2(6) | 0.424 0(3) | 0.788 3(1) |
| C(9) | 0.288 1(5) | 0.459 7(3) | 0.828 95(9) |
| C(10) | 0.232 7(5) | 0.388 5(2) | 0.871 49(9) |
| C(11) | 0.375 4(6) | 0.305 4(2) | 0.887 9(1) |
| C(12) | 0.320 4(7) | 0.241 5(3) | 0.926 5(1) |
| C(13) | 0.118 8(7) | 0.258 9(3) | 0.948 8(1) |
| C(14) | -0.023 8(7) | 0.342 6(3) | 0.933 1(1) |
| C(15) | 0.032 9(6) | 0.405 9(3) | 0.894 2(1) |
| O(16) | 0.516 1(4) | 0.448 6(2) | 0.816 62(7) |
| C(17) | -0.008 4(6) | 0.450 4(3) | 0.618 8(1) |
| C(18) | 0.005 9(6) | 0.469 6(3) | 0.572 8(1) |
| C(19) | -0.017 4(6) | 0.436 2(3) | 0.530 4(1) |
| C(20) | -0.227 4(6) | 0.387 5(3) | 0.531 7(1) |
| C(21) | -0.330 2(7) | 0.250 8(3) | 0.491 7(1) |
| C(22) | -0.225 0(8) | 0.363 0(3) | 0.449 9(1) |
| C(23) | -0.017 0(8) | 0.413 5(3) | 0.447 9(1) |
| C(24) | 0.087 3(7) | 0.450 7(3) | 0.487 7(1) |
| O(25) | 0.293 2(5) | 0.507 5(3) | 0.571 32(8) |

^a NH(1) and OH(16) coordinates:

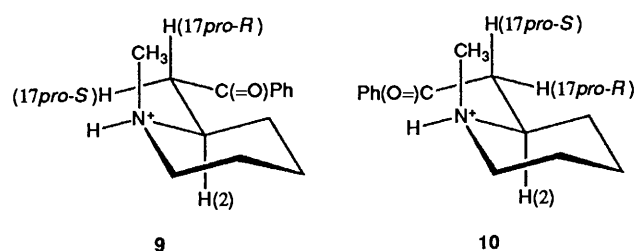
| | | | |
|-------|----------|----------|------------|
| H(1) | 0.100(6) | 0.357(3) | 0.700(1) |
| H(16) | 0.574(5) | 0.527(2) | 0.818 8(9) |

^b Equivalent coordinates [1.00 - x, 0.500 + y, 1.500 - z]:

| | | | |
|-------|-------------|-------------|------------|
| Br(a) | 0.686 13(5) | 0.714 00(8) | 0.820 7(1) |
|-------|-------------|-------------|------------|

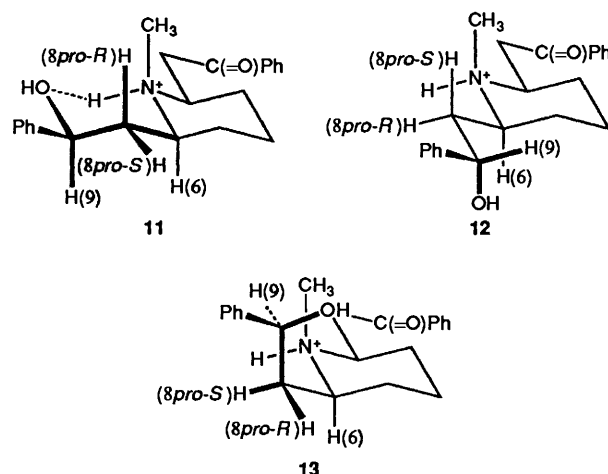
species relative to their C(5,6,8) counterparts in the phenethyl half. A similar finding was found for C(2,6) in the minor species. Thus, by analogy, the higher field resonances for the minor species C(3,5) and C(8,17) pairs were also assigned to nuclei residing in the acetophenonyl half.

Stereochemistry of Lobeline·HCl Major Species in CD₂Cl₂.—Vicinal *J*(HH) coupling constants involving protons ligated to C(2,3,5,6) and N(1) of the piperidine ring testify to a chair conformation in both species of the salt. The relative change in ¹³C NMR chemical shifts of externally diastereotopic nuclei in the two *N*-methyl epimers are also in agreement with an assignment of an axial *N*-methyl group in the major species and an equatorial one in the minor solution species. Carbons β to the methyl are shifted upfield in the axial *N*-methyl major species [C(2) and C(6) by 1.59 and 1.34 ppm, respectively]. There is a shift of 10.73 ppm upfield for the axial methyl carbon (relative to the equatorial one), while C(3) and C(5) in the γ -positions are characteristically shifted upfield by 5.62 and 6.69 ppm, respectively (the so-called ' γ -effect').¹³ The solid-state CP-MAS ¹³C NMR spectrum of crystalline 1a·HCl was recorded, and the methyl and C_{ipso} carbon atom resonances were assigned *via* a dipolar dephasing delay experiment based on less efficient solid-state relaxation¹⁴ for methyl carbons (*vis-à-vis* methylene and methine carbons).¹⁵ After a suitable delay period had been introduced prior to FID acquisition, methyl and quaternary carbon magnetization was still noted in the spectrum. Further confirmation of an axial *N*-methyl orientational assignment to the major solution-state species was obtained by comparison of root mean square (RMS) chemical shift differences between major and minor solution-state species *vs.* those of the solid-state [RMS differences of, respectively, 1.94 and 5.29 ppm for C(3,4,5,7)].



The observation of antiperiplanar-type 10.5 Hz and synclinal-type (*gauche*) 2.4 Hz magnitude coupling constants involving H(2) and the C(17)-methylene protons points to a preferred conformation about the major species C(2)–C(17) bond. Two models (9 and 10) for this arrangement differ by the fact that H(17*pro-S*) has a (+)-synclinal relationship to H(2) in 9, while H(17*pro-R*) has a (–)-synclinal relationship to H(2) in 10. Model 9 is similar to the X-ray determined conformation for the acetophenonyl arm, and was found to be relevant by means of an NOE intensity enhancement of *ca.* 5% noted for the 4.06 ppm H(17) resonance upon { δ 11.19, NH}. This finding also enabled assignment of *pro-S* and *pro-R* descriptors to the respective synclinal to H(2) and antiperiplanar to H(2) nuclei. The observation of an NOE is commensurate with the 2.363 Å NH...H(17*pro-S*) non-bonding distance in the X-ray structure of 1·HBr. Irradiation of major species NH also afforded NOE intensity enhancements to nearby H(2,6).

A second, preferred conformation is also seen for the C(8)–C(9) bond in the phenethyl moiety, since here too one observes antiperiplanar and synclinal magnitude vicinal coupling constants. Assignment of *pro-R* and *pro-S* descriptors to protons ligated to C(8) were made by recourse to molecular mechanics-calculated models of various phenethyl moiety conformations, *vide infra*. The 6–7 Hz vicinal coupling constant values involving the C(6)–C(8) bond clearly point to a weighted time-averaged interchange between three rotamers (11–13, where 11 and 12 are the same conformations found for crystalline 1·HCl·H₂O and 1·HBr, respectively). Using idealized 12 Hz antiperiplanar and 3 Hz synclinal coupling constant values, the equilibrium rotamer population may be estimated from the 6.8 Hz *J*(H6–H8*pro-R*) and 6.0 Hz *J*(H6–H8*pro-S*) values to be ~42% (11), ~33% (12) and ~25% (13). Molecular mechanics models of 11–13 also suggest the same 11 > 12 > 13 trend in fractional populations (models 12 and 13 are, respectively, 22.3 and 45.0 kJ higher than 11).



All three rotamers show the same invariant antiperiplanar H(9)...H(8*pro-R*) and (–)-synclinal H(9)...H(8*pro-S*) relationships as observed in solid-state structures 4–7. An alternative set of three rotameric models places H(9) anti-

Table 5 Non-hydrogen intramolecular and selected intermolecular bond distances and angles for (1*R*,2*R*,6*S*,C_β*S*)-(−)-α-lobeline hydrobromide (**1**·HBr); esds in parentheses refer to last digit printed

(a) Bond lengths/Å

| | | | |
|---------------|----------|----------------|----------|
| N(1)–C(2) | 1.531(4) | C(11)–C(12) | 1.387(4) |
| N(1)–C(6) | 1.525(4) | C(12)–C(13) | 1.388(6) |
| N(1)–C(7) | 1.504(4) | C(13)–C(14) | 1.380(6) |
| C(2)–C(3) | 1.516(4) | C(14)–C(15) | 1.391(5) |
| C(2)–C(17) | 1.524(4) | C(17)–C(18) | 1.517(5) |
| C(3)–C(4) | 1.508(5) | C(18)–C(19) | 1.486(5) |
| C(4)–C(5) | 1.515(4) | C(18)–O(25) | 1.211(5) |
| C(5)–C(6) | 1.517(4) | C(19)–C(20) | 1.386(5) |
| C(6)–C(8) | 1.527(4) | C(19)–C(24) | 1.400(5) |
| C(8)–C(9) | 1.524(4) | C(20)–C(21) | 1.381(5) |
| C(9)–C(10) | 1.525(4) | C(21)–C(22) | 1.376(5) |
| C(9)–O(16) | 1.422(4) | C(22)–C(23) | 1.384(7) |
| C(10)–C(11) | 1.382(4) | C(23)–C(24) | 1.383(5) |
| C(10)–C(15) | 1.384(5) | N(1)···Br | 3.199(2) |
| NH(1)···Br | 2.19(3) | N(1)–H(1) | 1.07(3) |
| O(16)···Br(a) | 3.274(2) | OH(16)···Br(a) | 2.30(3) |
| O(16)–H(16) | 0.98(3) | | |

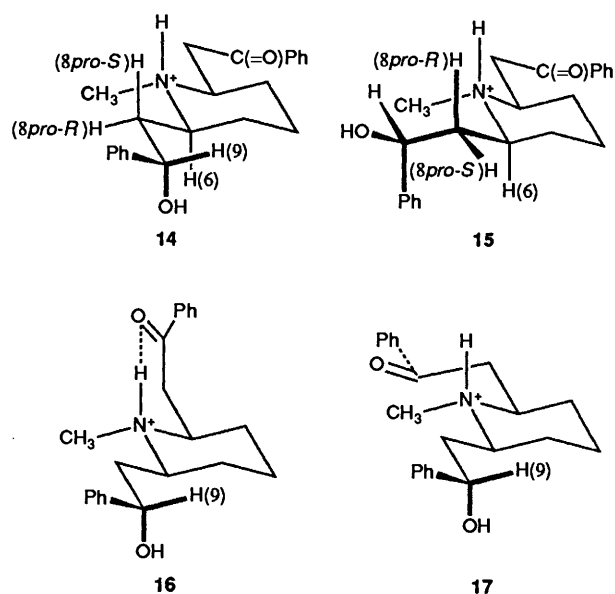
(b) Bond angles/°

| | | | |
|------------------|----------|---------------------|----------|
| C(2)–N(1)–C(6) | 110.5(2) | C(11)–C(10)–C(15) | 118.6(3) |
| C(2)–N(1)–C(7) | 113.3(2) | C(10)–C(11)–C(12) | 120.6(3) |
| C(6)–N(1)–C(7) | 114.4(2) | C(11)–C(12)–C(13) | 120.3(3) |
| N(1)–C(2)–C(3) | 111.0(2) | C(12)–C(13)–C(14) | 119.6(3) |
| N(1)–C(2)–C(17) | 110.4(2) | C(13)–C(14)–C(15) | 119.6(4) |
| C(3)–C(2)–C(17) | 114.4(3) | C(10)–C(15)–C(14) | 121.2(3) |
| C(2)–C(3)–C(4) | 111.2(3) | C(2)–C(17)–C(18) | 112.0(3) |
| C(3)–C(4)–C(5) | 111.3(3) | C(17)–C(18)–C(19) | 117.4(3) |
| C(4)–C(5)–C(6) | 111.3(2) | C(17)–C(18)–O(25) | 120.4(3) |
| N(1)–C(6)–C(5) | 110.9(2) | C(19)–C(18)–O(25) | 122.1(3) |
| N(1)–C(6)–C(8) | 110.1(2) | C(18)–C(19)–C(20) | 122.8(3) |
| C(5)–C(6)–C(8) | 115.8(2) | C(18)–C(19)–C(24) | 118.4(3) |
| C(6)–C(8)–C(9) | 113.0(3) | C(20)–C(19)–C(24) | 118.8(3) |
| C(8)–C(9)–C(10) | 110.5(2) | C(19)–C(20)–C(21) | 120.9(3) |
| C(8)–C(9)–O(16) | 109.4(2) | C(20)–C(21)–C(22) | 120.1(4) |
| C(10)–C(9)–O(16) | 111.4(2) | C(21)–C(22)–C(23) | 119.7(3) |
| C(9)–C(10)–C(11) | 121.8(3) | C(22)–C(23)–C(24) | 120.6(3) |
| C(9)–C(10)–C(15) | 119.5(3) | C(19)–C(24)–C(23) | 119.8(4) |
| N(1)–H(1)···Br | 156(3) | O(16)–H(16)···Br(a) | 175(2) |

periplanar and (+)-synclinal to H(8*pro-S*) and H(8*pro-R*), respectively. However, molecular mechanics calculations show these alternative models to be, respectively, 34.7, 15.8 and 17.4 kJ higher in energy than their 11–13 counterparts. Thus, the solid-state conformation about C(8)–C(9) was assigned as the putative solution-state conformation, and the 2.32₁ ppm proton ligated to C(8) was therefore assigned a *pro-R* descriptor.

Stereochemistry of Lobeline·HCl Minor Species in CD₂Cl₂.—The β-hydroxyphenethyl-moiety now appears to be the more rigid arm in the equatorial *N*-methyl minor species. This is seen by vicinal coupling constants involving the methylene protons ligated to C(8). Each of them is coupled to one synclinal and one antiperiplanar oriented neighbour. Two models (**14**, **15**) are consistent with these results, and each C(8)–C(9) bond conformational model has associated with it three C(2)–C(17) bond rotamers [as shown by time-averaged 5.1 Hz values for both *J*(H2–H17*pro-R*) and *J*(H2–H17*pro-S*)]. Molecular mechanics calculated models consistently showed lower energies for the H(8*pro-S*) synclinal to H(9) and H(8*pro-R*) antiperiplanar to H(9) arrangement (e.g. model **15** was found to be 17.7 kJ higher in energy than model **14**). On this basis, the 2.32₇ and 2.13 ppm C(8) methylene proton resonances were respectively assigned *pro-R* and *pro-S* descriptors.

The three C(2)–(17) bond rotamers for the acetophenonyl moiety are depicted in structures **14**, **16** and **17**. Again, using idealized 12 Hz antiperiplanar and 3 Hz synclinal coupling constant values, the equilibrium rotamer population may be



estimated from the two 5.1 Hz *J*(H2–H17*pro-R*) and *J*(H2–H17*pro-S*) values to be ~54% (**16**), ~23% (**17**) and ~23% (**14**). Molecular mechanics models of **14**, **16**, **17** also suggest the same **16** > **17** ≥ **14** trend in fractional populations (models **17** and **14** are, respectively, 24.1 and 25.8 kJ higher than **16**).

Stereochemistry of Lobeline·HCl in D₂O.—The aliphatic FEL ¹³C NMR spectral parameters of α-lobeline hydrochloride dissolved in D₂O show a clear similarity to those of the axial *N*-methyl diastereoisomer (**1a**·HCl) in CD₂Cl₂ (RMS difference of 9 values = 1.99 ppm vs. 5.91 ppm between those of the aqueous medium and those of the equatorial epimer **1e**·HCl). These similarities are especially observed in the resonances of γ-[C(3,5)] and methyl-[C(7)] carbons which are particularly sensitive¹³ to the axial/equatorial-orientation of the *N*-methyl group. Therefore, axial *N*-methyl diastereoisomer (**1a**·HCl) is the major contributor to the time-averaged FEL structure of α-lobeline hydrochloride in D₂O. While poor dispersion of ¹H NMR chemical shifts at 9.4 T prevented analysis of a number of multiplets, resonances involving the C(2)–C(17) and C(8)–C(9) bonds were found. Assuming the same *pro-R* and *pro-S* assignment for protons ligated to C(17) as found for **1a**·HCl at the SEL, the equilibrium rotamer population about the C(2)–C(17) bond may be estimated from the 9.2 Hz *J*(H2–H17*pro-R*) and 5.0 Hz *J*(H2–H17*pro-S*) homonuclear vicinal coupling constants to be ~69% [**9**, antiperiplanar angle N(1)–C(2)–C(17)–C(18)], ~22% [**10**, (–)-synclinal angle N(1)–C(2)–C(17)–C(18)], and ~9% [(+)-synclinal angle N(1)–C(2)–C(17)–C(18)]. Thus, the acetophenonyl arm appears to be more mobile in aqueous medium than in CD₂Cl₂, although the same major conformation (**9**) was seen in both solvents. Coupling constants involving the C(8)–C(9) bond can be interpreted as originating from antiperiplanar H(9)···H(8*pro-R*) and (–)-synclinal H(9)···H(8*pro-S*) dispositions similar to that observed for **1a,e**·HCl at the SEL.

Stereochemistry of Lobeline Free Base in CDCl₃.—Finally, the ¹³C NMR spectral parameters of free base **1** clearly show the existence of multiple species in both CDCl₃ and [2H₈]toluene. At least three species are present in spectra recorded at 4.7 and 5.85 T [e.g. CH₃ resonances (assigned by the DEPT sequence with 135° and 90° pulse widths): δ 27.18, 35.66 and 40.88 in the ratio ca. 17:5:4 at 298 K], while only one primary species plus traces of a second were ascertained in spectra recorded at 9.4 T (298 K) [e.g. CH₃ resonances: δ 27.33 and 35.69 (trace) at 298 K]. Ambient temperature spectra of free base **1** in either

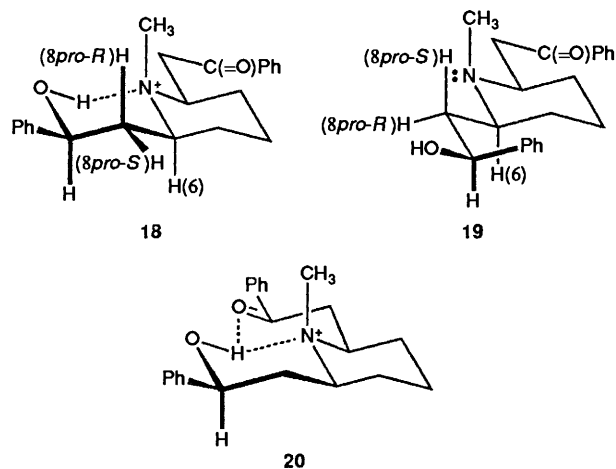
Table 6 Selected torsion angles (deg) for (1*R*,2*R*,6*S*,C₃*S*)-(-)- α -lobeline hydrobromide (1·HBr), and (-)- α -lobeline hydrochloride monohydrate (1·HCl·H₂O) in square brackets; esds in parentheses refer to last digit printed^a

| | | | |
|-------------------------|--------------------|-------------------------|--------------------|
| C(6)-N(1)-C(2)-C(3) | -56.0(2) [-59.6] | C(6)-N(1)-C(2)-C(17) | 176.1(3) [172.6] |
| C(7)-N(1)-C(2)-C(3) | 73.8(2) [67.0] | C(7)-N(1)-C(2)-C(17) | -54.1(2) [-60.8] |
| C(2)-N(1)-C(6)-C(5) | 55.9(2) [58.5] | C(2)-N(1)-C(6)-C(8) | -174.7(3) [-173.7] |
| C(7)-N(1)-C(6)-C(5) | -73.3(2) [-68.8] | C(7)-N(1)-C(6)-C(8) | 56.1(2) [58.9] |
| N(1)-C(2)-C(3)-C(4) | 56.1(2) [57.1] | C(17)-C(2)-C(3)-C(4) | -178.2(4) [-177.4] |
| N(1)-C(2)-C(17)-C(18) | -159.5(4) [-152.0] | C(3)-C(2)-C(17)-C(18) | 74.4(3) [82.4] |
| C(2)-C(3)-C(4)-C(5) | -55.9(2) [-52.3] | C(3)-C(4)-C(5)-C(6) | 55.9(2) [51.7] |
| C(4)-C(5)-C(6)-N(1) | -56.0(2) [-55.9] | C(4)-C(5)-C(6)-C(8) | 177.7(4) [175.6] |
| N(1)-C(6)-C(8)-C(9) | 177.5(3) [60.1] | C(5)-C(6)-C(8)-C(9) | -55.8(2) [-173.4] |
| C(6)-C(8)-C(9)-C(10) | -177.1(4) [162.3] | C(6)-C(8)-C(9)-O(16) | -54.2(3) [-74.3] |
| C(8)-C(9)-C(10)-C(11) | 107.7(3) [111.1] | C(8)-C(9)-C(10)-C(15) | -71.4(3) [-65.7] |
| O(16)-C(9)-C(10)-C(11) | -14.1(2) [-8.8] | O(16)-C(9)-C(10)-C(15) | 166.9(4) [174.4] |
| C(2)-C(17)-C(18)-C(19) | -173.6(4) [171.0] | C(2)-C(17)-C(18)-O(25) | 8.6(2) [-5.8] |
| C(17)-C(18)-C(19)-C(20) | -1.1(2) [41.4] | C(17)-C(18)-C(19)-C(24) | -178.5(4) [-139.5] |
| O(25)-C(18)-C(19)-C(20) | 176.7(5) [-141.9] | O(25)-C(18)-C(19)-C(24) | -0.7(2) [37.3] |

^a Values for six significantly different angles have been italicised; data for 1·HCl·H₂O was calculated from ref. 4.

CDCl₃ and [2H₈]toluene afford the same number of resonances and very similar chemical shifts. Chemical shifts of free base (**1**) major species carbons are very similar to those noted for the axial *N*-methyl species of **1a**·HCl in CD₂Cl₂ [RMS differences for the nine aliphatic carbons are 1.88 (**1** vs. **1a**·HCl) and 5.19 (**1** vs. **1e**·HCl)]. Again, these similarities are especially apparent in the γ -[C(3,5)] and methyl-[C(7)] carbon chemical shifts [*i.e.* RMS differences of corresponding C(3,5,7) resonances are 0.28 ppm (**1** vs. **1a**·HCl) and 8.03 ppm (**1** vs. **1e**·HCl)]. Therefore, the major free base species also appears to have an axial *N*-methyl group, while the lower field values for the two minor species may be assigned to putative equatorial *N*-methyl isomers. More work is needed to firmly determine the identity of the two minor species. Variable-temperature ¹³C NMR experiments on **1** in [2H₈]toluene showed intensity changes testifying to relative population changes within the equilibrium of three species [*e.g.* the δ 26.15 CH₃ species is preponderant at 304 K (and below), while the δ 34.32 CH₃ species becomes predominant at 314 K (and above)]. No evidence for coalescence or marked line-broadening was noted up to and including 354 K.

The ¹H NMR spectrum of free base **1** in CDCl₃ shows the presence of one time-averaged species. The β -hydroxyphenethyl-moiety appears to be fairly conformationally constrained due to the finding of antiperiplanar and synclinal magnitude coupling constants for both C(6)-C(8) and C(8)-C(9) bonds. Depending on the 8*pro-R*/8*pro-S* descriptor assignment, two models (**18**, **19**) may again explain the observation that one of the methylene protons is mutually antiperiplanar to H(6) and H(9). Molecular mechanics calculations show model **19** to be 16.7 kJ higher in energy than **18**. The δ 1.94 proton was



therefore putatively assigned a *pro-R* descriptor since the anti-periplanar H(9)···H(8*pro-R*)/(-)-synclinal H(9)···H(8*pro-S*) disposition is (a) the lower energy arrangement for the C(8)-C(9) bond (similar to other cases discussed above), and (b) structure **18** shows the presence of an internal hydrogen-bond.

The acetophenonyl arm shows a mixture of conformations as judged from H(2) coupling constants to the C(17)-methylene protons. However, the appropriate 17*pro-R*/17*pro-S* descriptors cannot be unequivocally ascertained by spectroscopy alone. Using the 8.2 and 5.0 Hz coupling constant values, the fractional populations of **18** and **20** are either, respectively, ~22% and ~58% [if $\delta_H(17*pro-R*) = 3.03$] or, respectively, ~58% and ~22% [if $\delta_H(17*pro-R*) = 3.23$], while the (+)-synclinal angle N(1)-C(2)-C(17)-C(18) rotamer is ~20% in both cases. A point in favour of the first assignment is that a *pro-R* descriptor was also assigned to the higher field H(17) resonance in the case of **1e**·HCl, and 1·HCl interconverting C(2)-C(17) bond rotamers. Moreover, the $\delta_H(17*pro-R*) = 3.03$ assignment is also consistent with molecular mechanics calculations showing **18** to be 2.6 kJ higher in energy than the bifurcated hydrogen-bonded **20**.

Bioactive Conformation of Lobeline Salts.—A model for the bioactive conformation of nicotine agonists was made by Sheridan, Dixon and co-workers¹⁶ using an ensemble approach to distance geometry. In this model for the nicotinic pharmacophore, three essential groups in each agonist were defined as a cationic centre (A), an electronegative atom (B), and an atom (C) that forms a dipole with B.¹⁵ The pharmacophore for the superimposition of these groups in a series of nicotinic agonists consisted of a triangle with sides 4.8 Å (A···B), 4.0 Å (A···C), and 1.2 Å (B···C).¹⁵ The averaged values in the 1·HCl·H₂O and 1·HBr X-ray structures are, respectively, 4.18(1) Å [A···B = N···O(25)], 3.82(3) Å [A···C = N···C(18)], and 1.212(1) Å [B···C = C(18)-O(25)]. The carbonyl group approximately eclipses the C(2)-C(17) bond in both structures. Molecular mechanics exploration of the proposed model for the bioactive conformation afforded a suitable candidate whose primary difference *vs.* the two X-ray structures is carbonyl group coplanarity with the C(2)-C(3) bond [*i.e.* -1(7)° C(3)-C(2)···C(18)-O(25)]. Starting from either initial 1·HCl·H₂O or 1·HBr X-ray geometries, similar putative bioactive conformational minima were found exhibiting the following averaged characteristic torsion angles: -167(2)° N(1)-C(2)-C(17)-C(18), -75(1)° C(2)-C(17)-C(18)-O(25), -33(1)° O(25)-C(18)-C(19)-C(24), and 106(1)° C(2)-C(17)-C(18)-C(19). These models were calculated to be 10.2 and 15.9 kJ higher in energy than the respective energy-minimized 1·HCl·H₂O and 1·HBr X-ray geometries, and the

sides of the proposed pharmacophoric triangle were 4.54(2) Å (A...B), 3.89(1) Å (A...C) and 1.22 Å (B...C).

Experimental

Crystallography.— α -Lobeline hydrochloride (Fluka AG) $\{[\alpha]_D^{20} -57^\circ (c = 2, \text{H}_2\text{O}), \text{lit.},^1 [\alpha]_D^{20} -43^\circ (c = 2, \text{H}_2\text{O})\}$ was dissolved in water, converted into the free base with excess KOH solution, and extracted with chloroform. The combined organic layers were dried over anhydrous MgSO_4 , filtered, and evaporated under reduced pressure to dryness. A white solid separated after treatment of the free base in diethyl ether with ethereal HBr. Dissolution of the solid in absolute ethanol followed by vapour diffusion of acetone yielded clear, colourless, crystalline prisms, belonging to the orthorhombic system $P2_12_12_1$, melting point 206.0–206.5 °C (decomp.) (uncorrected). Intensity data were collected at 293 K on an Enraf-Nonius CAD-4 automatic diffractometer. Table 3 provides crystallographic and data collection details. The NRCVAX programs¹⁷ were used for centering, indexing and data collection. The unit cell dimensions were obtained by a least-squares fit of 24 centred reflections in the range of $60^\circ \leq 2\theta \leq 100^\circ$. Reflections were measured with a constant speed of 2.7 deg min⁻¹. During data collection, the intensities of two standard reflections were monitored every 60 min. No significant decay was observed.

The structure was solved by the application of direct methods and refined by least squares using the NRCVAX program.¹⁷ An isotropic extinction coefficient was included in the refinement¹⁸ to account for secondary extinction effects;¹⁹ its value was 1.49(4). Atomic scattering factors stored in the NRCVAX program were those of Cromer and Waber.²⁰ Hydrogens were geometrically placed with the exception of O–H, which was found in the difference-Fourier map, and refined isotropically while all other non-hydrogen atoms were refined anisotropically. At convergence the final discrepancy indices on F were $R(F) = 0.030$ and $R_w(F) = 0.022$ for the 2130 reflections with $I_{\text{net}} \geq 2.0\sigma(I_{\text{net}})$ and 236 variables.*

The residual negative and positive electron densities in the final map were $-0.47 \text{ e } \text{Å}^{-3}$ and $0.38 \text{ e } \text{Å}^{-3}$. The maximum shift/ σ was 0.022. The NRCVAX version of the Bijvoet method was utilized to determine the absolute configuration.⁸ Based on 80 measurements of Friedel pairs, 71 support the (1*R*,2*R*,6*S*,*C*_β*S*)-model. Thus, the probability that the above statement is wrong is 0.22×10^{-12} .

NMR.—¹H (9.4, 11.7 T) and ¹³C (4.7, 5.9, 9.4 T) NMR spectra [CD_2Cl_2 and D_2O (for the HCl salt), CDCl_3 (for the free base), sealed 5 mm sample tube, 298 K] were obtained at 400.1 and 500.1 MHz [¹H] and 50.3, 62.9, 100.1 MHz [¹³C] on the appropriate Bruker WP-200-SY, WM-250, AM-400, AM-500 and Varian VXR-400S Fourier transform spectrometers. The deuterated solvent was used as an internal lock, and residual protio CDHCl_2 solvent was used as an internal secondary reference for spectra of the HCl salt recorded in CD_2Cl_2 [δ_{H} 5.32 and δ_{C} 53.8 relative to tetramethylsilane]. For spectra of the HCl salt recorded in D_2O , 3-(methylsilyl)-1-propanesulfonic acid, sodium salt, was used as an external reference, while tetramethylsilane was used as an internal reference for spectra of the free base [ambient temperature (CDCl_3) and 50.3 MHz ¹³C NMR variable temperature ($[\text{C}_6\text{H}_6]$ toluene)]. Standard Varian microprograms were used for the DEPT (90°

and 135° pulse angles), difference NOE (NOEDIFF), difference homonuclear decoupling, COSY-90, and XHCORR experiments. Solid-state ¹³C NMR (75.3 MHz) were recorded on a Chemagnetics CMX Fourier transform spectrometer operating in the CP-MAS mode using cross polarization *via* spinlock with bilevel decoupling. Hexamethylbenzene (17.4 ppm) was used as an external secondary reference for the solid-state spectra. An evolution delay period of 40 μs was used in solid-state dipolar dephasing experiments.

Molecular Mechanics.—The minimized energy geometries of the molecular mechanics-calculated model compounds were determined by the MMX subprogram within PCMOD 4.25,²¹ performed on a Macintosh SE/30 equipped with a RasterOps SE/30 colour board/RGB colour monitor. MMX is an enhanced version of Allinger's MM2 program²² with MMP1 π -subroutines²³ incorporated for localized π -electron systems. Non-iconic molecular graphics were drawn with the BALL & STICK 3.0 program.²⁴

Acknowledgements

Gratitude is expressed to Dr. Claude Nissim Cohen (Ciba-Geigy AG) for hospitality extended to R. G. during a recent summer sabbatical visit. Thanks are given to Dr. Hanspeter Sauter (Ciba-Geigy AG) for helpful discussions, and for use of 9.4 T high-field Varian NMR instrumentation. Acknowledgement is also made for a 11.7 T ¹H NMR spectrum recorded by Dr. Michael J. Shapiro (Sandoz USA), 5.9 T ¹³C NMR spectra recorded by Mr. Serge Bérubé (Université de Sherbrooke), and 7.0 T CP-MAS ¹³C NMR spectra recorded by Dr. Fred Morin (McGill University). Appreciation is also extended to Dr. George Francis (University of Bergen) for the gift of (–)- α -lobeline hydrochloride, and to the Kreitman Family Endowment Fund, Ben-Gurion University of the Negev, for the purchase of a Bruker WP-200-SY FT-NMR spectrometer.

References

- 1 *The Merck Index*, ed. S. Budavari, Merck, Rahway, 11th edn., 1989, p. 873, and references therein.
- 2 C. Schoepf and E. Mueller, *Justus Liebigs Ann. Chem.*, 1965, **687**, 241.
- 3 R. B. Barlow and O. Johnson, *Br. J. Pharmacol.*, 1989, **98**, 799.
- 4 R. Glaser, J.-P. Charland and A. Michel, *J. Chem. Soc., Perkin Trans. 2*, 1989, 1875.
- 5 P. J. Pauling and T. J. Petcher, *J. Chem. Soc., Chem. Commun.*, 1969, 1001.
- 6 R. Glaser, Q.-J. Peng and A. S. Perlin, *J. Org. Chem.*, 1988, **53**, 2172, and references therein.
- 7 J. Feeney, R. Foster and E. A. Piper, *J. Chem. Soc., Perkin Trans. 2*, 1977, 2016.
- 8 J. M. Bijvoet, A. F. Peerdeman and A. J. Bommel, *Nature (London)*, 1951, **168**, 271.
- 9 C. Schoepf, G. Dummer, W. Wust and R. Rausch, *Justus Liebigs Ann. Chem.*, 1959, **626**, 134.
- 10 C. Hootelé, B. Colau, F. Halin, J. P. Declercq, G. Germain and M. van Meerssche, *Tetrahedron Lett.*, 1980, **21**, 5063.
- 11 C. Hootelé, B. Colau, F. Halin, J. P. Declercq, G. Germain and M. van Meerssche, *Tetrahedron Lett.*, 1980, **21**, 5061.
- 12 L. F. Johnson and W. C. Jankowski, *Carbon-13 NMR Spectra—A Collection of Assigned, Coded, and Indexed Spectra*, Wiley-Interscience, New York, 1972.
- 13 D. K. Dalling and D. M. Grant, *J. Am. Chem. Soc.*, 1974, **96**, 1827 and references therein.
- 14 (a) S. K. Opella and G. J. Frey, *J. Am. Chem. Soc.*, 1979, **101**, 5854; (b) S. J. Opella, G. J. Frey and B. P. Cross, *J. Am. Chem. Soc.*, 1979, **101**, 5856.
- 15 R. Glaser, Q.-J. Peng and A. S. Perlin, *J. Org. Chem.*, 1988, **53**, 2172 and references therein.
- 16 R. P. Sheridan, R. Nilakantan, J. S. Dixon and R. Venkataraghavan, *J. Med. Chem.*, 1986, **29**, 899.

* The final discrepancy index $R(F)$ is defined as: $R(F) = (\sum_i |F_{\text{obs},i} - |F_{\text{calc},i}||) / (\sum_i |F_{\text{obs},i}|)$; the weighted value R_w is defined as: $R_w(F) = [(\sum_i w_i (|F_{\text{obs},i} - |F_{\text{calc},i}||)^2) / (\sum_i w_i (|F_{\text{obs},i}|)^2)]^{1/2}$ and the particular weighting factor used, w_i , is given in Table 3.

- 17 E. J. Gabe, F. L. Lee and Y. LePage, *The NRCVAX Crystal Structure System in Crystallographic Computing*. In *Data Collection, Structure Determination, Proteins and Data Bases*, eds. G. M. Sheldrick, C. Kruger and R. Goddard, Clarendon Press, Oxford, 1985, vol. 3, pp. 167–174.
- 18 A. C. Larson, *Acta Crystallogr.*, 1967, **23**, 664.
- 19 W. H. Zachariasen, *Acta Crystallogr.*, 1963, **16**, 1139.
- 20 D. T. Cromer and J. T. Waber, in *International Tables for X-Ray Crystallography*, eds. J. A. Ibers and W. C. Hamilton, Kynoch Press, Birmingham, 1974; vol. IV; pp. 99–101, Table 2.2B. (Present distributor, Kluwer Academic Publishers, Dordrecht, The Netherlands).
- 21 PCMOD/MMX 4.25, Serena Software Inc., POB 3076, Bloomington, Indiana, USA.
- 22 N. L. Allinger, *J. Am. Chem. Soc.*, 1977, **99**, 8127.
- 23 N. L. Allinger and J. T. Sprague, *J. Am. Chem. Soc.*, 1973, **95**, 3893.
- 24 BALL & STICK 3.0, Cherwell Scientific Publishing Ltd, Oxford, UK.

Paper 2/01019D

Received 26th February 1992

Accepted 18th March 1992